Appl. Phys. B 79, 95–98 (2004)
DOI: 10.1007/s00340-004-1489-3

Applied Physics B
Lasers and Optics

H.Y. TANG✉
W.H. WONG
E.Y.B. PUN

Long period polymer waveguide grating device with positive temperature sensitivity

Department of Electronic Engineering, City University of Hong Kong, Tat Chee Avenue, Hong Kong

Received: 15 December 2003
Published online: 30 March 2004 •

ABSTRACT A long-period waveguide grating (LPWG) was demonstrated in a low-loss negative tone UV-sensitive epoxy novolak resin polymer. The grating structure was fabricated on top of the waveguide using a standard UV lithography process, and no other subsequent process is required after the development step. It is shown that with an appropriate design of the structure a transmission peak at the desired wavelength can be achieved. The LPWG exhibits an attenuation of −18 dB using a grating length of 17 mm. The temperature sensitivity of the LPWG is linear and is found to be ∼ 0.89 nm/°C. A red shift of the transmission peak wavelength was also observed and is discussed.

PACS 42.70.Jk; 42.79.Dj; 42.79.Gn

1 Introduction

Long-period gratings (LPGs) in optical fibers are useful and versatile devices. Gain equalizers for broad-band amplifiers [1] and band-rejection filters [2], and optical fiber polarizers [3], have been demonstrated, as well as sensors for strain, temperature [4, 5], and refractive index [6]. UV irradiation is required to create an absorption defect due to the photosensitivity of the fiber, resulting in the generation of modulation gratings inside the fiber core. Because the fiber is normally round in shape and made of silica, the structural flexibility of the final device is limited. To circumvent the geometry and material constraints of an optical fiber, long-period gratings have been implemented in planar optical waveguides recently [7], and LPGs can be fabricated in different shapes with different waveguide materials.

Polymeric optical waveguides are attractive for telecommunication applications, because of their simple processing steps and low production costs compared to silica-based materials. Polymer materials can be molecularly engineered [8, 9] and fine tuning of the optical properties is possible. Also, polymer waveguide devices can be integrated with other optical components on the same substrate to form new functional planar lightwave circuits.

✉ Fax: +852-2788-7791, E-mail: eeeybpun@cityu.edu.hk

The key requirements imposed on the polymer materials are low losses, good processability, good adhesion to the substrate, environmental stability, and long-term thermal stability. For these reasons, a negative tone epoxy novolak resin (ENR) polymer (formally named NANO^{TM} SU8 2000) from MicroChem Corp. was chosen. ENR polymer is sensitive to UV exposure, and no other subsequent process is required after the development step. Other properties of ENR [10], such as high refractive index (∼ 1.57 at 1.55 μm), large hardness (∼ 0.3–0.6 G Pa), and high glass-transition temperature ($T_g > 200$ °C) for fully cross linking make it attractive for waveguide applications.

The long-period waveguide grating (LPWG) transmission spectrum can be tailored [7]. However, the grating structures were fabricated in the substrate by etching through a UV-defined photoresist mask. This method involves many processing steps and can lead to a long fabrication. In this work, we report using a standard UV exposure technique to fabricate the long-period gratings in a planar polymer waveguide. A UV-sensitive polymer material with a high refractive index is used as both the waveguide and grating layers. Double exposure was used and no etching step is required; hence the processing time is reduced. A chrome-plated amplitude mask with designated patterns was used to define the channel width and the grating periodicity. The performances of the LPWGs were investigated as well as their temperature dependence.

2 Device fabrication

Figure 1 shows the schematic diagram of the fabrication procedures for the polymeric LPWG devices. Negative tone epoxy novolak resin polymer ∼ 2.5-μm thick was first spun on thermally oxidized silicon wafers as the waveguide layer, and a pre-exposure bake time of 5 min at 90 °C was applied to the samples. Channel stripe patterns were fabricated in the waveguide layer by a standard UV lithography process. After exposure through the photomask the samples were developed for 15 s in propyleneglycol-monomethyletheracetate (PGMEA) and then rinsed in fresh PGMEA again to form the stripe waveguides. Next, the channel waveguides were covered with ENR polymer again, and similar pre-exposure, baking, and UV exposure conditions were used to form the corrugated grating patterns on the top of the channel waveguides. Finally, the samples were covered with

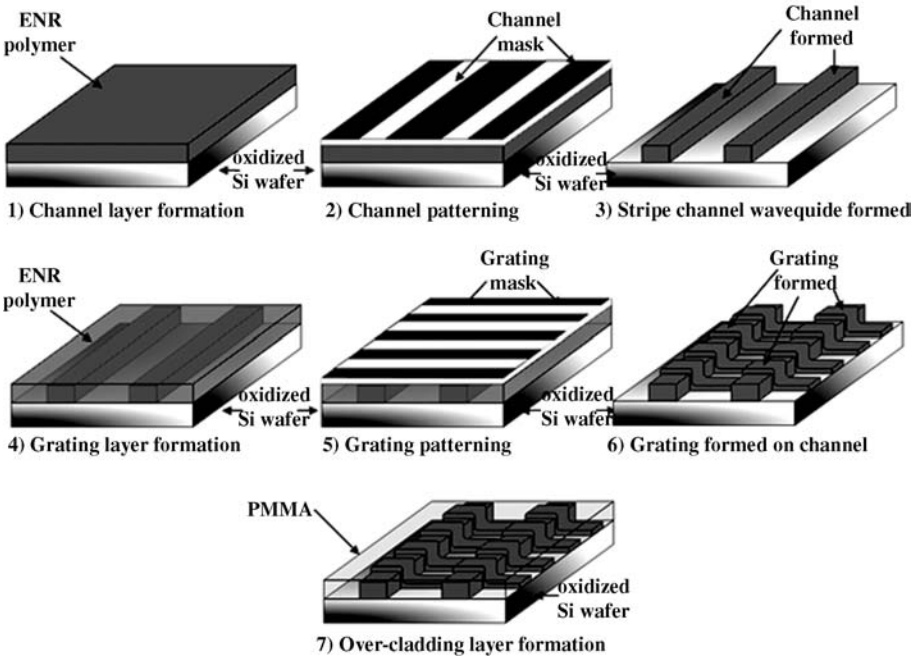

FIGURE 1 Schematic diagram of the LPWG fabrication procedures

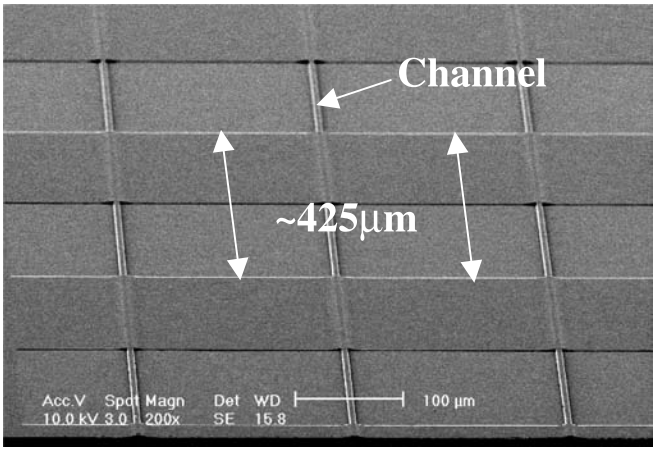

FIGURE 2 SEM image of a 6-μm channel waveguide with grating patterns on top

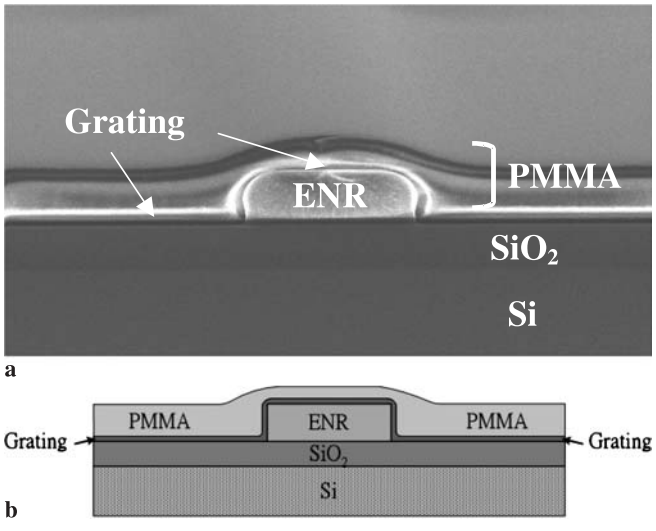

FIGURE 3 **a** SEM image of the cross section of a 6-μm-wide channel waveguide with grating patterns on top and covered by an over-cladding; **b** corresponding schematic diagram

an over-cladding layer of polymethylmethacrylate (PMMA) with a thickness of ∼ 3 μm in order to protect the gratings, and buried channel waveguides with long-period periodic structures on top were obtained. Figure 2 shows a scanning electron microscopy (SEM) image of the LPWG viewed from the top without the upper cladding. The channel is 6-μm wide and the grating pattern appears on top of the waveguide; the peak-to-peak grating height is ∼ 300 nm. The depth of the grating is controlled by the spinning speed, and the grating periodicity is controlled by the designed amplitude mask. Figure 3 shows both the SEM image and the corresponding schematic diagram of the cross section of the LPWG. It can be seen that the waveguide cross section has been slightly modified due to the stress induced by the over-cladding layer.

3 Results and discussion

3.1 *Spectral response of LPWG devices*

In order to characterize the LPWG device, either an erbium-doped fiber amplifier (EDFA) operating at the ∼ 1.5-μm-wavelength band or a broad-band superluminescent light-emitting diode operating at around the 1.3-μm-wavelength band was adopted. Both end faces of the LPWG were butt coupled to single-mode optical fibers to enable light to be launched into and out of the device, and the transmitted light was recorded using an optical spectrum analyzer (OSA).

A normalized transmission spectrum of the LPWG is depicted in Fig. 4. As shown in Fig. 4a, a transmission peak of ∼ −13 dB at 1.5-μm wavelength was observed with a grating period of 425 μm, corresponding to an attenuation of > 95%. In Fig. 4b, a transmission peak of ∼ −18 dB at 1.3-μm wavelength was observed with a grating period of 400 μm, corresponding to an attenuation of > 98%. As shown in Fig. 4a, the side lobe is ∼ − 1.8 dB of the grating, and is prone to noise resulting from the coupling condition of light into the LPWG and losses induced by the fabrication process. To circumvent

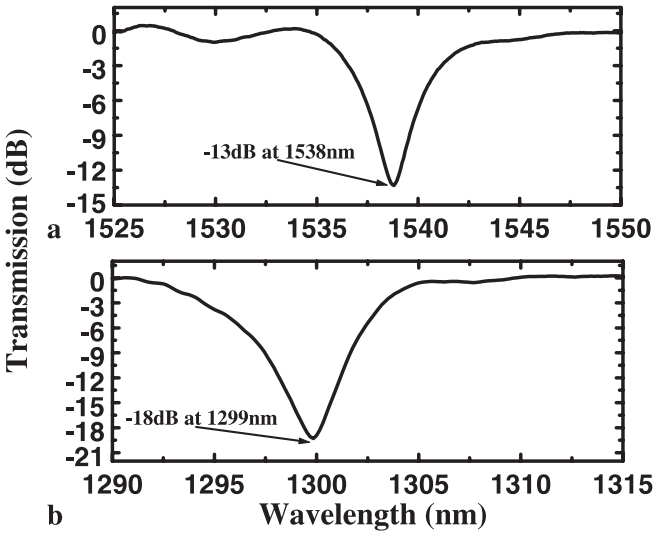

FIGURE 4 Transmission spectrum of LPWG at **a** 1.5-μm wavelength and **b** 1.3-μm wavelength

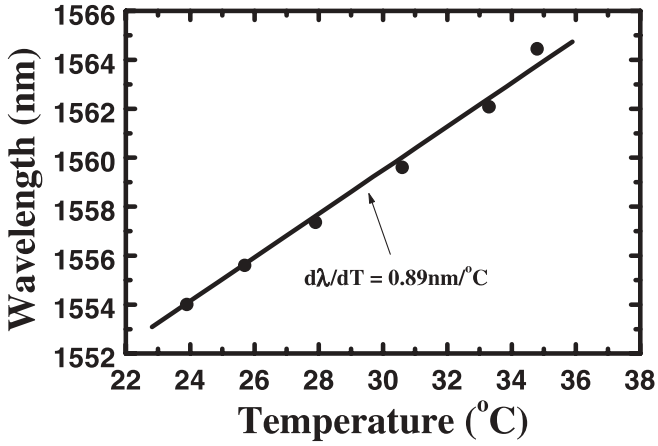

FIGURE 5 Dependence of LPWG transmission peak wavelength on temperature

this problem, both the coupling condition and the fabrication process were optimized, and the side lobe can be minimized, as shown in Fig. 4b. With an appropriate design of the structure, a transmission peak operating at the desired wavelength can be achieved.

3.2 *Thermal response of LPWG devices*

The temperature dependence of the transmission peak wavelength in a LPWG is due to thermal expansion and thermo-optic effects. Mode coupling takes place at a peak wavelength λ_p given by the phase-matching condition [2]

$$\lambda_p = \Lambda[N_w(\lambda) - N_c(\lambda)]\,, \tag{1}$$

where Λ is the grating period and $N_w(\lambda)$ and $N_c(\lambda)$ are the effective indices of the waveguide mode and the cladding mode, respectively. The value of $N_w(\lambda)$ depends on the waveguide and cladding refractive indices, while $N_c(\lambda)$ depends on the waveguide, cladding, and surrounding region indices [11]. By differentiating (1) with respect to temperature (T), the temperature dependence of the transmission peak wavelength can be expressed as [4]

$$\frac{d\lambda_p}{dT} \approx \Lambda\left[\frac{dN_w(\lambda)}{dT} - \frac{dN_c(\lambda)}{dT}\right]. \tag{2}$$

Hence, $d\lambda_p/dT$ can either be positive or negative, that is, the transmission peak can be red shifted or blue shifted.

The thermal response of the LPWG was also characterized by heating the sample from 24 °C to 36 °C with an incremental step of 0.2-mA current using a temperature-controllable thermoelectric heater. The accuracy of the temperature measurement is 0.1 °C, and it took about 10 min for the sample to reach the desired temperature in each incremental step. Figure 5 shows the dependence of transmission peak wavelength on temperature. The transmission peak wavelength shifts toward longer wavelength as the temperature increases and is linear, indicating that the thermally induced peak wavelength exhibits a red-shift performance. A total of ∼ 10.4-nm peak wavelength shift was obtained for such a small temperature range, achieving a temperature sensitivity of ∼ 0.89 nm/°C. In Table 1, the thermal responses of Long Period Fibre Gratings (LPFGs) and LPWGs are shown. The value for our LPWG is higher than those reported for LPFGs using standard telecommunication fiber [5, 14], and is similar to those reported using special fibers: the fibers were either recoated or had polymer incorporated [15].

Polymer material generally shows a negative thermo-optic coefficient. By using a Metricon 2010 prism coupler system, the thermo-optic coefficients (dn/dT) of ENR and PMMA were measured. As shown in Fig. 6a and b, the values are $\sim -1.75 \times 10^{-4}$ and $\sim -1.0 \times 10^{-4}$, respectively. The value for PMMA is very close to the value reported in the literature [12]. The effective refractive index of the waveguide $N_w(\lambda)$ is determined from the waveguide and the cladding indices n_w and n_c, which means that N_w changes with n_c. When the cladding has a negligible thermo-optic coefficient, the change in N_w due to thermally induced refractive-index change in the cladding is negligible compared to that of the waveguide. According to (2), a shift in transmission peak

Application of LPG	Temp. sensitivity $d\lambda/dT$ (nm/°C)	Wavelength shift $\Delta\lambda$ (nm)	Temp. range ΔT (°C)
LPWG [this work]	∼ 0.89	10.4	12
Gain-flattening filter [16]	∼ 0.46	35	76
Band-rejection filter [17]	0.63	37.8	60
Tunable filter [15]	0.8	50	60
Strain and temp. sensing [4]	0.28	36.4	130

TABLE 1 Comparison between thermal responses of LPFGs and LPWGs

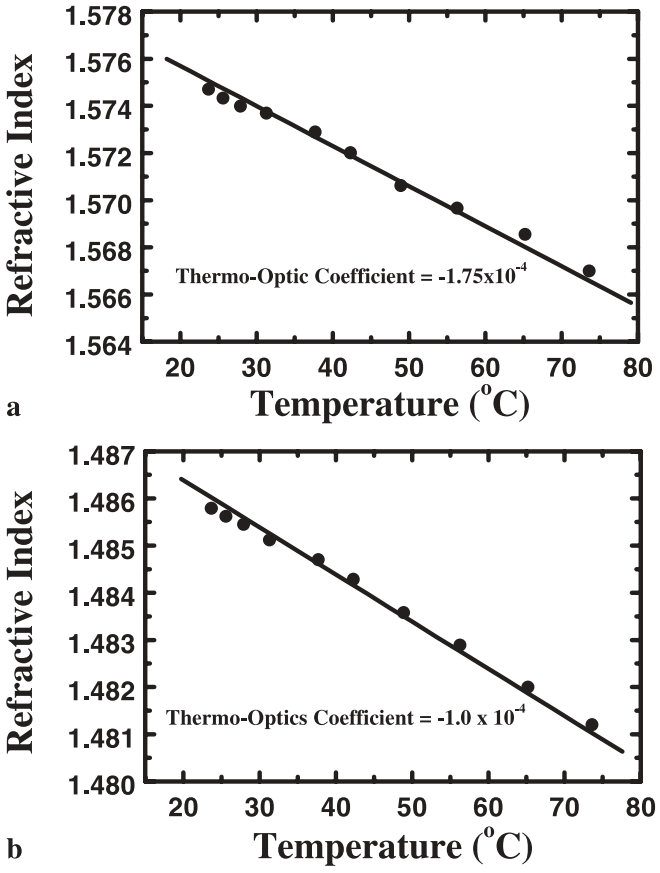

FIGURE 6 Variations in refractive index as a function of temperature measured at 1550-nm wavelength: **a** ENR polymer and **b** PMMA polymer

wavelength with respect to temperature can be determined by the difference in the change of effective index due to the thermally induced refractive-index changes of the material. A reduction in the index difference, $N_w - N_c$, with respect to temperature, will result in shifting to shorter wavelength upon heating. By referring to [7], as the SiO_2 cladding has a negligible thermo-optic coefficient [13], the change in N_w depends mainly on the thermally induced refractive-index change of ENR. As dn/dT of ENR has a negative slope, a reduction of N_w will result. Thus, a blue shift of the peak wavelength is observed.

In this work, the PMMA polymer cladding has a higher thermo-optic coefficient compared with that of SiO_2; hence the change in N_w of an ENR waveguide will not only be influenced by the thermally induced refractive-index change of ENR, but also the index change of PMMA. This phenomenon is similar to the reported result using polymer over-cladding to reduce the change in effective index of the waveguide [13]. From (2) a red shift of the peak wavelength can be achieved if the difference in the change of effective index of the waveguide and the cladding is expanded. Because the magnitude of the effective index change of ENR is smaller than that of PMMA, a red shift of peak wavelength was observed for the LPWG.

4 Conclusions

In conclusion, LPWGs based on UV-sensitive ENR polymer materials were demonstrated. Both the waveguide and the grating layers use the same polymer material, and the double-exposure process is relatively simple compared to other fabrication methods. No other subsequent process such as reactive ion etching is required, and the grating-fabrication errors can be minimized. The LPWGs exhibit an attenuation of ~ -18 dB using a grating length of 17 mm and a peak-to-peak depth of 300 nm. The temperature sensitivity of the LPWGs is ~ 0.89 nm/°C and is higher than and similar to the values reported for LPFGs using standard silica fibers and special fibers, respectively. LPWGs are attractive, exhibiting a relatively small size and a similar performance to LPFGs, and will be useful for telecommunication and sensor applications.

ACKNOWLEDGEMENTS This work is supported by the Research Grants Council of the Hong Kong Special Administrative Region, China, under Grant Project CityU 1194/02E. The authors are grateful to H.C. Tsoi and K.K. Tung for useful discussions, and the EPA Centre, City University of Hong Kong, for help in obtaining the SEM images.

REFERENCES

1 A.M. Vengsarkar, J.R. Pedrazzani, J.B. Judkins, P.J. Lemaire, N.S. Bergano, C.R. Davidson: Opt. Lett. **21**, 336 (1996)
2 A.M. Vengsarkar, P.J. Lemaire, J.B. Judkins, V. Bhatia, T. Erdogab, J.E. Sipe: J. Lightwave Technol. **14**, 58 (1996)
3 B. Ortega, L. Dong, W.F. Liu, J.P. de Sandro, L. Reekie, S.I. Tsypina, V.N. Bagratashvili, R.I. Lamming: IEEE Photon. Technol. Lett. **9**, 1370 (1997)
4 Y. Han, C.S. Kim, U.C. Paek, Y. Chung: IEICE Trans. Electron. **e83-c**, 282 (2000)
5 V. Bhatia, A.M. Vengsarkar: Opt. Lett. **21**, 692 (1996)
6 H.J. Patrick, G.M. Williams, A.D. Kersey, F. Bucholtz: J. Lightwave Technol. **16**, 1606 (1998)
7 H.C. Tsoi, W.H. Wong, E.Y.B. Pun: IEEE Photon. Technol. Lett. **15**, 721 (2003)
8 K.D. Singer, M.G. Kuzyk, J.E. Sohn: J. Opt. Soc. Am. B **4**, 968 (1987)
9 S.J. Lalama, A.F. Garito: Phys. Rev. A **20**, 1179 (1979)
10 W.H. Wong, J. Zhou, E.Y.B. Pun: Appl. Phys. Lett. **78**, 2110 (2001)
11 A. Abramov, B.J. Eggleton, J.A. Rogers, R.P. Espindola, A. Hale, R.S. Windeler, T.A. Strasser: IEEE Photon. Technol. Lett. **11**, 445 (1999)
12 H.Y. Liu, G.D. Peng, P.L. Chu: IEEE Photon. Technol. Lett. **13**, 824 (2001)
13 Y. Kokubum, M. Takizawa, S. Taga: Electron. Lett. **30**, 1223 (1994)
14 M. Shigehara, T. Enomoto, S. Ishikawa, M. Harumoto, H. Kanamori: in *APCC/OECC'99, Beijing, 1999*, p. 1610
15 A. Abramov, A. Hale, R.S. Windeler, T.A. Strasser: Electron. Lett. **35**, 81 (1999)
16 J.K. Bae, S.H. Kim, J.H. Kim, J. Bae, S.B. Lee, J.M. Jeong: IEEE Photon. Technol. Lett. **15**, 407 (2003)
17 C.G. Atherton, A.L. Steele, J.E. Hoad: IEEE Photon. Technol. Lett. **12**, 65 (2000)